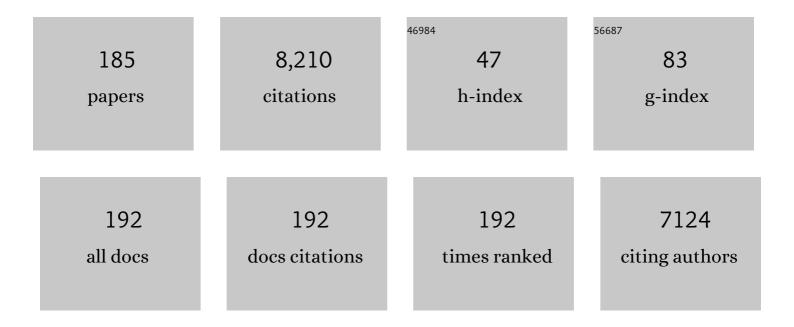
List of Publications by Year in descending order

Source: https://exaly.com/author-pdf/660372/publications.pdf Version: 2024-02-01



Erneluo

#	Article	IF	CITATIONS
1	UTSA-74: A MOF-74 Isomer with Two Accessible Binding Sites per Metal Center for Highly Selective Gas Separation. Journal of the American Chemical Society, 2016, 138, 5678-5684.	6.6	489
2	Amyloid fibril structure of α-synuclein determined by cryo-electron microscopy. Cell Research, 2018, 28, 897-903.	5.7	339
3	Synthesis of novel nanomaterials and their application in efficient removal of radionuclides. Science China Chemistry, 2019, 62, 933-967.	4.2	256
4	Photoswitching CO ₂ Capture and Release in a Photochromic Diarylethene Metal–Organic Framework. Angewandte Chemie - International Edition, 2014, 53, 9298-9301.	7.2	238
5	Hydrothermal Synthesis of Metalâ~'Organic Frameworks Based on Aromatic Polycarboxylate and Flexible Bis(imidazole) Ligands. Crystal Growth and Design, 2008, 8, 606-611.	1.4	232
6	Ammoniating Covalent Organic Framework (COF) for Highâ€Performance and Selective Extraction of Toxic and Radioactive Uranium Ions. Advanced Science, 2019, 6, 1900547.	5.6	200
7	A robust Th-azole framework for highly efficient purification of C2H4 from a C2H4/C2H2/C2H6 mixture. Nature Communications, 2020, 11, 3163.	5.8	192
8	Atomic structures of FUS LC domain segments reveal bases for reversible amyloid fibril formation. Nature Structural and Molecular Biology, 2018, 25, 341-346.	3.6	185
9	Metal–organic framework (MOF): lanthanide(iii)-doped approach for luminescence modulation and luminescent sensing. Dalton Transactions, 2010, 39, 4485.	1.6	163
10	Ultrafast high-performance extraction of uranium from seawater without pretreatment using an acylamide- and carboxyl-functionalized metal–organic framework. Journal of Materials Chemistry A, 2015, 3, 13724-13730.	5.2	161
11	Structural basis for reversible amyloids of hnRNPA1 elucidates their role in stress granule assembly. Nature Communications, 2019, 10, 2006.	5.8	157
12	High-performance Hg ²⁺ removal from ultra-low-concentration aqueous solution using both acylamide- and hydroxyl-functionalized metal–organic framework. Journal of Materials Chemistry A, 2015, 3, 9616-9620.	5.2	151
13	Functionalizing the pore wall of chiral porous metal–organic frameworks by distinct –H, –OH, –NH2, –NO2, –COOH shutters showing selective adsorption of CO2, tunable photoluminescence, and direct white-light emission. Chemical Communications, 2012, 48, 5989.	2.2	145
14	Significant Enhancement of C ₂ H ₂ /C ₂ H ₄ Separation by a Photochromic Diarylethene Unit: A Temperature―and Lightâ€Responsive Separation Switch. Angewandte Chemie - International Edition, 2017, 56, 7900-7906.	7.2	145
15	The application of single-crystal-to-single-crystal transformation towards adjustable SMM properties. Chemical Communications, 2012, 48, 1006-1008.	2.2	131
16	Direct extraction of U(VI) from alkaline solution and seawater via anion exchange by metal-organic framework. Chemical Engineering Journal, 2017, 316, 154-159.	6.6	128
17	Trinuclear Cobalt Based Porous Coordination Polymers Showing Unique Topological and Magnetic Variety upon Different Dicarboxylate-like Ligands. Crystal Growth and Design, 2009, 9, 1066-1071.	1.4	127
18	Coumarin-modified microporous-mesoporous Zn-MOF-74 showing ultra-high uptake capacity and photo-switched storage/release of UVI ions. Journal of Hazardous Materials, 2016, 311, 30-36.	6.5	126

#	Article	IF	CITATIONS
19	Engineering design toward exploring the functional group substitution in 1D channels of Zn–organic frameworks upon nitro explosives and antibiotics detection. Dalton Transactions, 2018, 47, 5359-5365.	1.6	126
20	Unprecedented (3,4)-connected metal–organic frameworks (MOFs) with 3-fold interpenetration and considerable solvent-accessible void space. Chemical Communications, 2007, , 3744.	2.2	110
21	The MOF ⁺ Technique: A Significant Synergic Effect Enables High Performance Chromate Removal. Angewandte Chemie - International Edition, 2017, 56, 16376-16379.	7.2	102
22	Synthesis, Structure, and Characterization of Three Series of 3d–4f Metal-Organic Frameworks Based on Rod-Shaped and (6,3)-Sheet Metal Carboxylate Substructures. Chemistry - A European Journal, 2007, 13, 4948-4955.	1.7	99
23	Selective extraction of thorium from uranium and rare earth elements using sulfonated covalent organic framework and its membrane derivate. Chemical Engineering Journal, 2020, 384, 123240.	6.6	96
24	Pillared 3dâ^'4f Frameworks with Rare 3D Architecture Showing the Coexistence of Ferromagnetic and Antiferromagnetic Interactions between Gadolinium Ions. Crystal Growth and Design, 2007, 7, 851-853.	1.4	84
25	Employing La2- (La = Eu, Tb, Pr) or Co3-Based Molecule Building Blocks To Construct 3,8-Connected Nets: Hydrothermal Synthesis, Structure, Luminescence, and Magnetic Properties. Crystal Growth and Design, 2008, 8, 2006-2010.	1.4	84
26	A Variety of 1D to 3D Metalâ^'Organic Coordination Architectures Assembled with 1,1′-(2,2′-Oxybis(ethane-2,1-diyl))bis(1 <i>H</i> -imidazole). Crystal Growth and Design, 2008, 8, 1654-1662	. 1.4	83
27	Photoswitching adsorption selectivity in a diarylethene–azobenzene MOF. Chemical Communications, 2017, 53, 763-766.	2.2	80
28	Using MOF-74 for Hg2+ removal from ultra-low concentration aqueous solution. Journal of Solid State Chemistry, 2017, 246, 16-22.	1.4	79
29	Metal-organic framework (MOF) showing both ultrahigh As(V) and As(III) removal from aqueous solution. Journal of Solid State Chemistry, 2019, 269, 264-270.	1.4	78
30	U(VI) adsorption onto covalent organic frameworks-TpPa-1. Journal of Solid State Chemistry, 2019, 277, 484-492.	1.4	76
31	Parkinson's disease associated mutation E46K of α-synuclein triggers the formation of a distinct fibril structure. Nature Communications, 2020, 11, 2643.	5.8	76
32	The First Self-Penetrating Topology Based on an Unusual α-Po Net with Double Edges Constructed from a 12-Connected Gd2(μ2-Ocarboxylate)2(μ2-OH2)2(μ3-OH)2Cu2 Core. Crystal Growth and Design, 2006, 6, 2432-2434.	1.4	73
33	Construction of Lanthanide Metalâ^'Organic Frameworks by Flexible Aliphatic Dicarboxylate Ligands Plus a Rigid <i>m</i> -Phthalic Acid Ligand. Crystal Growth and Design, 2007, 7, 1733-1737.	1.4	71
34	Novel azo-Metal–Organic Framework Showing a 10-Connected bct Net, Breathing Behavior, and Unique Photoswitching Behavior toward CO ₂ . Inorganic Chemistry, 2015, 54, 11587-11589.	1.9	65
35	Tunable perylene-based donor-acceptor conjugated microporous polymer to significantly enhance photocatalytic uranium extraction from seawater. Chemical Engineering Journal, 2021, 412, 127558.	6.6	64
36	Constructing redox-active microporous hydrogen-bonded organic framework by imide-functionalization: Photochromism, electrochromism, and selective adsorption of C2H2 over CO2. Chemical Engineering Journal, 2020, 383, 123117.	6.6	63

#	Article	IF	CITATIONS
37	An unusual metal–organic framework showing both rotaxane- and cantenane-like motifs. CrystEngComm, 2008, 10, 981.	1.3	62
38	Constructing Well-Defined and Robust Th-MOF-Supported Single-Site Copper for Production and Storage of Ammonia from Electroreduction of Nitrate. ACS Central Science, 2021, 7, 1066-1072.	5.3	59
39	Structure-Based Peptide Inhibitor Design of Amyloid-β Aggregation. Frontiers in Molecular Neuroscience, 2019, 12, 54.	1.4	58
40	Adsorption equilibrium and kinetics of uranium onto porous azo-metal–organic frameworks. Journal of Radioanalytical and Nuclear Chemistry, 2016, 310, 353-362.	0.7	56
41	Anchoring nZVI on metal-organic framework for removal of uranium(â¥) from aqueous solution. Journal of Solid State Chemistry, 2019, 269, 16-23.	1.4	56
42	Ultralow-Content Iron-Decorated Ni-MOF-74 Fabricated by a Metal–Organic Framework Surface Reaction for Efficient Electrocatalytic Water Oxidation. Inorganic Chemistry, 2019, 58, 11500-11507.	1.9	55
43	Constructing bimetal-complex based hydrogen-bonded framework for highly efficient electrocatalytic water splitting. Applied Catalysis B: Environmental, 2019, 258, 117973.	10.8	55
44	Robust metal–organic framework with multiple traps for trace Xe/Kr separation. Science Bulletin, 2021, 66, 1073-1079.	4.3	55
45	Flexible and robust bimetallic covalent organic frameworks for the reversible switching of electrocatalytic oxygen evolution activity. Journal of Materials Chemistry A, 2020, 8, 5907-5912.	5.2	50
46	A novel 2D→3D array in a vertical mode containing both polyrotaxane and polycatenane motifs. CrystEngComm, 2012, 14, 5714.	1.3	49
47	General Strategy to Fabricate Metal-Incorporated Pyrolysis-Free Covalent Organic Framework for Efficient Oxygen Evolution Reaction. Inorganic Chemistry, 2020, 59, 4995-5003.	1.9	49
48	Insight into volatile iodine uptake properties of covalent organic frameworks with different conjugated structures. Journal of Solid State Chemistry, 2019, 279, 120979.	1.4	48
49	Hierarchical Ni ₂ P@NiFeAlO _{<i>x</i>} Nanosheet Arrays as Bifunctional Catalysts for Superior Overall Water Splitting. Inorganic Chemistry, 2019, 58, 3247-3255.	1.9	47
50	Multifunctional 3-Fold Interpenetrated Porous Metal–Organic Frameworks Composed of Unprecedented Self-Catenated Networks. Crystal Growth and Design, 2012, 12, 3392-3396.	1.4	46
51	Removal and safe reuse of highly toxic allyl alcohol using a highly selective photo-sensitive metal–organic framework. Green Chemistry, 2016, 18, 2047-2055.	4.6	46
52	Stable Iron Hydroxide Nanosheets@Cobaltâ€Metal–Organic–Framework Heterostructure for Efficient Electrocatalytic Oxygen Evolution. ChemSusChem, 2019, 12, 4623-4628.	3.6	46
53	Five porous zinc(<scp>ii</scp>) coordination polymers functionalized with amide groups: cooperative and size-selective catalysis. Journal of Materials Chemistry A, 2015, 3, 20210-20217.	5.2	43
54	MOF catalysis of Fe ^{II} -to-Fe ^{III} reaction for an ultrafast and one-step generation of the Fe ₂ O ₃ @MOF composite and uranium(<scp>vi</scp>) reduction by iron(<scp>ii</scp>) under ambient conditions. Chemical Communications, 2016, 52, 9538-9541.	2.2	43

#	Article	IF	CITATIONS
55	Functionalizing a Metal–Organic Framework by a Photoassisted Multicomponent Postsynthetic Modification Approach Showing Highly Effective Hg(II) Removal. Inorganic Chemistry, 2018, 57, 8722-8725.	1.9	43
56	A Ternary Metalâ^'Organic Framework Built on Triangular Organic Spacers, Square and Tetrahedral Co ₂ Secondary Building Units. Crystal Growth and Design, 2008, 8, 176-178.	1.4	42
57	Highly efficient transfer hydrodeoxygenation of vanillin over Sn4+-induced highly dispersed Cu-based catalyst. Applied Surface Science, 2019, 480, 548-556.	3.1	42
58	Carboxylate-assisted acylamide metal–organic frameworks: synthesis, structure, thermostability and luminescence studies. CrystEngComm, 2012, 14, 6182.	1.3	38
59	Chiral 1D Dy(iii) compound showing slow magnetic relaxation. Dalton Transactions, 2011, 40, 12651.	1.6	37
60	MOF surface method for the ultrafast and one-step generation of metal-oxide-NP@MOF composites as lithium storage materials. Journal of Materials Chemistry A, 2016, 4, 13603-13610.	5.2	37
61	Beyond Crystal Engineering: Significant Enhancement of C ₂ H ₂ /CO ₂ Separation by Constructing Composite Material. Inorganic Chemistry, 2018, 57, 3679-3682.	1.9	35
62	Chiral or achiral camphorate-based complexes controlled by the conformational rigidity of N-donor co-ligands. CrystEngComm, 2010, 12, 2769.	1.3	34
63	A self-catenated network containing unprecedented 0D + 2D → 2D polycatenation array. Dalton Transactions, 2012, 41, 11559.	1.6	34
64	Promising long-lasting phosphor material: a novel metal–organic framework showing intriguing luminescent performance. Dalton Transactions, 2012, 41, 13280.	1.6	34
65	lsoreticular MOFs functionalized in the pore wall by different organic groups for high-performance removal of uranyl ions. Journal of Radioanalytical and Nuclear Chemistry, 2016, 310, 317-327.	0.7	34
66	Photoswitching storage of guest molecules in metal–organic framework for photoswitchable catalysis: exceptional product, ultrahigh photocontrol, and photomodulated size selectivity. Journal of Materials Chemistry A, 2017, 5, 7961-7967.	5.2	34
67	Boosting Selective Adsorption of Xe over Kr by Double-Accessible Open-Metal Site in Metal–Organic Framework: Experimental and Theoretical Research. Inorganic Chemistry, 2020, 59, 11793-11800.	1.9	34
68	Unique Anionic Eight-Connected Net with 36418536 Topology Derived from a Rare Co6(μ3-OH)2(μ-H2O)(CO2)12 Building Block. Crystal Growth and Design, 2009, 9, 1271-1274.	1.4	32
69	Grafting functional groups in metal–organic frameworks for U(<scp>vi</scp>) sorption from aqueous solutions. Dalton Transactions, 2020, 49, 12536-12545.	1.6	32
70	Lanthanide separation using size-selective crystallization of Ln-MOFs. Chemical Communications, 2017, 53, 5737-5739.	2.2	31
71	A Zinc MOF with Carboxylate Oxygenâ€Functionalized Pore Channels for Uranium(VI) Sorption. European Journal of Inorganic Chemistry, 2019, 2019, 735-739.	1.0	31
72	Two new metal–triazole-benzenedicarboxylate frameworks affording an uncommon 3,4-connected net and unique 4,6-connected rod packing: hydrothermal synthesis, structure, thermostability and luminescence studies. CrystEngComm, 2009, 11, 1097.	1.3	30

#	Article	IF	CITATIONS
73	Reversible photo/thermoswitchable dual-color fluorescence through single-crystal-to-single-crystal transformation. Dalton Transactions, 2017, 46, 338-341.	1.6	29
74	Sulfonated perylene-based conjugated microporous polymer as a high-performance adsorbent for photo-enhanced uranium extraction from seawater. Polymer Chemistry, 2021, 12, 867-875.	1.9	29
75	Construction of Cu(II)–Gd(III) metal–organic framework by the introduction of a small amino acid molecule: hydrothermal synthesis, structure, thermostability, and magnetic studies. CrystEngComm, 2008, 10, 1613.	1.3	28
76	Metal-organic framework containing both azo and amide groups for effective U(VI) removal. Journal of Solid State Chemistry, 2018, 265, 148-154.	1.4	28
77	Ultralow-Content Palladium Dispersed in Covalent Organic Framework for Highly Efficient and Selective Semihydrogenation of Alkynes. Inorganic Chemistry, 2019, 58, 10829-10836.	1.9	28
78	Heat shock protein 104 (HSP104) chaperones soluble Tau via a mechanism distinct from its disaggregase activity. Journal of Biological Chemistry, 2019, 294, 4956-4965.	1.6	28
79	Employing An Unprecedented Ferromagnetic Molecular Building Block (MBB) of [Co2Ln(μ3-OH)(CO2)5(N3)]2 (Ln = Tb, Gd, Dy, Eu, Sm) to Construct a 6-Connected α-Po Net. Crystal Growth and Design, 2008, 8, 3508-3510.	1.4	27
80	One-Pot Synthesis of Schiff-Base-Containing Ni ₈ Clusters:  Solvothermal Synthesis, Structure, and Magnetic Properties. Inorganic Chemistry, 2007, 46, 8448-8450.	1.9	26
81	Three-dimensional graphene oxide/phytic acid composite for uranium(VI) sorption. Journal of Radioanalytical and Nuclear Chemistry, 2015, 306, 507-514.	0.7	26
82	Pd@Zn-MOF-74: Restricting a Guest Molecule by the Open-Metal Site in a Metal–Organic Framework for Selective Semihydrogenation. Inorganic Chemistry, 2018, 57, 12444-12447.	1.9	26
83	A Ni/Fe complex incorporated into a covalent organic framework as a single-site heterogeneous catalyst for efficient oxygen evolution reaction. Inorganic Chemistry Frontiers, 2020, 7, 3925-3931.	3.0	25
84	Robust Th-MOF-Supported Semirigid Single-Metal-Site Catalyst for an Efficient Acidic Oxygen Evolution Reaction. ACS Catalysis, 2022, 12, 9101-9113.	5.5	25
85	Size-selective catalysts in five functionalized porous coordination polymers with unsaturated zinc centers. New Journal of Chemistry, 2017, 41, 12611-12616.	1.4	24
86	Enhancing C ₂ H ₂ /C ₂ H ₄ separation by incorporating low-content sodium in covalent organic frameworks. Inorganic Chemistry Frontiers, 2019, 6, 2921-2926.	3.0	24
87	Rational tuning of thorium-organic frameworks by reticular chemistry for boosting radionuclide sequestration. Nano Research, 2022, 15, 1472-1478.	5.8	24
88	Rod-packing motif: a new metal–organic polymer showing unusual rod-packing architecture. CrystEngComm, 2011, 13, 44-46.	1.3	23
89	Solvent-induced supramolecular isomers, structural diversity, and unprecedented in situ formation of both inorganic and organic ions in inorganic–organic mercury(ii) complexes. Dalton Transactions, 2012, 41, 12670.	1.6	23
90	Programming Conventional Electron Microscopes for Solving Ultrahigh-Resolution Structures of Small and Macro-Molecules. Analytical Chemistry, 2019, 91, 10996-11003.	3.2	23

#	Article	IF	CITATIONS
91	Rare Three-Dimensional Uranyl–Biphenyl-3,3′-disulfonyl-4,4′-dicarboxylate Frameworks: Crystal Structures, Proton Conductivity, and Luminescence. Inorganic Chemistry, 2020, 59, 2952-2960.	1.9	23
92	Carambola-like metal-organic frameworks for high-performance electrocatalytic oxygen evolution reaction. Journal of Energy Chemistry, 2021, 53, 358-363.	7.1	23
93	Temperature-controlled structure diversity observed in the Zn(ii)-oxalate-4,4′-bipyridine three-member system. CrystEngComm, 2010, 12, 1750.	1.3	22
94	Significant Enhancement of C ₂ H ₂ /C ₂ H ₄ Separation by a Photochromic Diarylethene Unit: A Temperature―and Lightâ€Responsive Separation Switch. Angewandte Chemie, 2017, 129, 8008-8014.	1.6	22
95	High Adsorption Capacity and Selectivity of SO ₂ over CO ₂ in a Metal–Organic Framework. Inorganic Chemistry, 2021, 60, 4-8.	1.9	22
96	Rarely Decorated Rutile Frameworks Built from Triangular Organic Spacers and Distorted Octahedral Co3 Building Blocks. European Journal of Inorganic Chemistry, 2007, 2007, 3906-3910.	1.0	21
97	Multi-functional magnetic, ferroelectric, and fluorescent homochiral lanthanide (Ln)–camphorate compounds built on helical {Ln–O}n inorganic substructures. CrystEngComm, 2011, 13, 6827.	1.3	21
98	The first 2D→3D polycatenation array built on (3,4)-connected bilayer nets. CrystEngComm, 2012, 14, 7861.	1.3	21
99	Heteroatom engineering of polymeric carbon nitride heterojunctions for boosting photocatalytic reduction of hexavalent uranium. Molecular Systems Design and Engineering, 2020, 5, 882-889.	1.7	21
100	Simple Method and Materials to Target Co(II)-Dy(III) Multi-Nuclear Magnetic Compounds and Single Molecule Magnets (SMMs): Synthesis, Structure, and Magnetic Studies. Australian Journal of Chemistry, 2013, 66, 75.	0.5	20
101	Photo-responsive azo MOF exhibiting high selectivity for CO ₂ and xylene isomers. Journal of Coordination Chemistry, 2016, 69, 1179-1187.	0.8	20
102	Construction of Metal-Organic Frameworks with the Pyridine-3,5-dicarboxylate Anion and Bis(imidazole) Ligands: Synthesis, Structure, and Thermostability Studies. European Journal of Inorganic Chemistry, 2010, 2010, 5592-5596.	1.0	19
103	Second messenger Ap4A polymerizes target protein HINT1 to transduce signals in FcεRl-activated mast cells. Nature Communications, 2019, 10, 4664.	5.8	19
104	Ultrahigh uranium extraction performance of COFs/SPES mixed matrix membranes at acidic medium. Journal of Solid State Chemistry, 2020, 288, 121364.	1.4	19
105	A Robust Cage-Based Metal–Organic Framework Showing Ultrahigh SO ₂ Uptake for Efficient Removal of Trace SO ₂ from SO ₂ /CO ₂ and SO ₂ /CO ₂ /N ₂ Mixtures. Inorganic Chemistry, 2021, 60, 3447-3451.	1.9	19
106	A novel partially open state of SHP2 points to a "multiple gear―regulation mechanism. Journal of Biological Chemistry, 2021, 296, 100538.	1.6	18
107	Solvent-induced reversible single-crystal-to-single-crystal transformations observed in lanthanide complexes. Dalton Transactions, 2013, 42, 8545.	1.6	17
108	Hybrid Catalyst of a Metal–Organic Framework, Metal Nanoparticles, and Oxide That Enables Strong Steric Constraint and Metal–Support Interaction for the Highly Effective and Selective Hydrogenation of Cinnamaldehyde. Inorganic Chemistry, 2018, 57, 12461-12465.	1.9	17

#	Article	IF	CITATIONS
109	High-performance removal of mercury ions (II) and mercury vapor by SO3â^'-anchored covalent organic framework. Journal of Solid State Chemistry, 2020, 282, 121126.	1.4	17
110	Structural Evolution from Noninterpenetrated to Interpenetrated Thorium–Organic Frameworks Exhibiting High Propyne Storage. Inorganic Chemistry, 2021, 60, 6472-6479.	1.9	16
111	Employing Cd–O–C rod-shaped secondary building units to construct 2D metal-organic frameworks (MOFs): hydrothermal synthesis, structures, and luminescent properties. Journal of Coordination Chemistry, 2008, 61, 2097-2104.	0.8	15
112	A series of 1D Dy(iii) compound showing slow magnetic relaxation: synthesis, structure, and magnetic studies. Dalton Transactions, 2012, 41, 6749.	1.6	15
113	A novel acylamide MOF showing self-catenated hxg-d-4-Fddd nets with 3-fold interpenetration and highly selective adsorption of CO2 over N2, CH4, and CO. Inorganic Chemistry Communication, 2014, 49, 56-58.	1.8	15
114	A new azo metal-organic framework showing polycatenated 3D array and ultrahigh U(VI) removal. Journal of Solid State Chemistry, 2018, 266, 244-249.	1.4	15
115	A [Th ₈ Co ₈] Nanocage-Based Metal–Organic Framework with Extremely Narrow Window but Flexible Nature Enabling Dual-Sieving Effect for Both Isotope and Isomer Separation. CCS Chemistry, 2022, 4, 1016-1027.	4.6	15
116	Three new acylamide ligands formed in situ and their application in constructing metal–organic frameworks. CrystEngComm, 2012, 14, 8418.	1.3	14
117	Optimization of Reaction Conditions towards Multiple Types of Framework Isomers and Periodicâ€Increased Porosity: Luminescence Properties and Selective CO ₂ Adsorption over N ₂ . ChemPhysChem, 2013, 14, 3594-3599.	1.0	14
118	Exceptional temperature-dependent coordination sites from acylamide groups. Dalton Transactions, 2014, 43, 5260.	1.6	14
119	Constructing various metal–organic frameworks by mixed pyridine–acylamide and carboxylate ligands: ring-like or helical building blocks. CrystEngComm, 2014, 16, 7440-7451.	1.3	14
120	Robust 4d–5f Bimetal–Organic Framework for Efficient Removal of Trace SO ₂ from SO ₂ /CO ₂ and SO ₂ /CO ₂ /N ₂ Mixtures. Inorganic Chemistry, 2021, 60, 1310-1314.	1.9	14
121	Creating and tailoring ultrathin two-dimensional uranyl-organic framework nanosheets for boosting photocatalytic oxidation reactions. Applied Catalysis B: Environmental, 2021, 297, 120485.	10.8	14
122	New topology observed in highly rare interlaced triple-stranded molecular braid. CrystEngComm, 2011, 13, 421-425.	1.3	13
123	Framework isomers controlled by the speed of crystallization: different aggregation fashions of Zn(ii) and 1,2,4-triazol-3-amine, distinct (3,4)-connected self-penetrating nets, and various pore shapes. Dalton Transactions, 2013, 42, 13802.	1.6	13
124	Decorated rutile net built on the six-connected Ln2 SBUs (secondary building units) and three-connected organic spacers. Inorganic Chemistry Communication, 2008, 11, 711-713.	1.8	12
125	Highly Rare Ferromagnetic Interaction with the Cu(tetrahedron)-Cu(square)-Cu(tetrahedron) Mode Observed in A 2-Fold Interpenetrating Moganite Net. Crystal Growth and Design, 2009, 9, 2047-2049.	1.4	12
126	A microporous metal–organic framework containing an exceptional four-connecting 4264topology and a combined effect for highly selective adsorption of CO2over N2. Dalton Transactions, 2013, 42, 50-53.	1.6	12

#	Article	IF	CITATIONS
127	Modulation of experimental conditions towards generation of a heterometallic Na2Co4 cluster or a homometallic Co4 cluster and ligand formed in situ. CrystEngComm, 2014, 16, 2570.	1.3	12
128	Urothermal synthesis of mononuclear lanthanide compounds: slow magnetization relaxation observed in Dy analogue. CrystEngComm, 2014, 16, 585-590.	1.3	12
129	The MOF ⁺ Technique: A Significant Synergic Effect Enables High Performance Chromate Removal. Angewandte Chemie, 2017, 129, 16594-16597.	1.6	12
130	Applying MOF ⁺ technique for <i>in situ</i> preparation of a hybrid material for hydrogenation reaction. Dalton Transactions, 2018, 47, 14889-14892.	1.6	12
131	Construction and modulation of structural diversity in acylamide-MOFs. CrystEngComm, 2014, 16, 5608-5618.	1.3	11
132	General Approach for Constructing Mechanoresponsive and Redox-Active Metal–Organic and Covalent Organic Frameworks by Solid–Liquid Reaction: Ferrocene as the Versatile Function Unit. Inorganic Chemistry, 2020, 59, 5271-5275.	1.9	10
133	Synthesis, Characterization, and Electrocatalytic Activity Exploration of MOF-74: A Research-Style Laboratory Experiment. Journal of Chemical Education, 2021, 98, 3341-3347.	1.1	10
134	A new Zn-triazole MOF showing very long-lived luminescence up to 3Â s. Journal of Solid State Chemistry, 2021, 301, 122369.	1.4	10
135	A highly twisting chiral qtz-d net built on a distorted tetrahedral node containing two types of helical substructure. Inorganic Chemistry Communication, 2011, 14, 1815-1818.	1.8	9
136	[Zn5(PO4)(HPO4)4(Hbpy)2(bpy)][H2PO4]·H2O: a novel inorganic–organic metal-phosphate framework showing an unprecedented (3,4)-connected (4·62)6(4·62·103)2(64·102)2 topology and the coexistence of various phosphates. CrystEngComm, 2012, 14, 5730.	1.3	9
137	The MOF ⁺ Technique: A Potential Multifunctional Platform. Chemistry - A European Journal, 2018, 24, 13701-13705.	1.7	9
138	Constructing a robust gigantic drum-like hydrophobic [Co24U6] nanocage in a metal–organic framework for high-performance SO2 removal in humid conditions. Journal of Materials Chemistry A, 2021, 9, 4075-4081.	5.2	9
139	A coordination polymer with a (3,4)-connected (4 <b<math>\hat{A}-6²)₂(4²) Tj ET</b<math>	Qq1 1 0.7 0.8	784314 rg ^B 8
	luminescent properties. Journal of Coordination Chemistry, 2008, 61, 363-371.		
140	Constructing PtI@COF for semi-hydrogenation reactions of phenylacetylene. Journal of Solid State Chemistry, 2020, 285, 121176.	1.4	8
141	Creating uniform pores for xenon/ krypton and acetylene/ethylene separation on a strontium-based metal-organic framework. Journal of Solid State Chemistry, 2020, 288, 121337.	1.4	8
142	Synthesis, crystal structure, and magnetic properties of a new end-to-end thiocyanato-bridged dicobalt(II) complex CoII(dien)(H2O)(NCS)(μ1,3-NCS)CoII(dien)(NCS)2 (dien = diethylenetriamine). Journal of Coordination Chemistry, 2010, 63, 610-616.	0.8	7
143	Construction of structural diversity and fine-tuned porosity in acylamide MOFs by a synthetic approach. New Journal of Chemistry, 2016, 40, 2021-2027.	1.4	7
144	Azo-MOFs showing controllable framework flexibility and consequently fine-tuned photomechanical crystal motion. Journal of Solid State Chemistry, 2019, 277, 182-186.	1.4	7

#	Article	IF	CITATIONS
145	Classified Encapsulation of an Organic Dye and Metal–Organic Complex in Different Molecular Compartments for White-Light Emission and Selective Adsorption of C2H2 over CO2. Inorganic Chemistry, 2021, 60, 8211-8217.	1.9	7
146	A robust metal-organic framework showing two distinct pores for effective separation of xenon and krypton. Microporous and Mesoporous Materials, 2021, 326, 111350.	2.2	7
147	A Robust Calcium–Organic Framework for Effective Separation of Xenon and Krypton. Crystal Growth and Design, 2021, 21, 954-959.	1.4	7
148	Hydrothermal synthesis and crystal structure of a metal–organic compound with unique pseudo-hexagonal water channels: [Cull(phen)(sal)]·0.5H2O (phen=1,10-phenanthroline, sal=salicylic) Tj ETQq0	0008gBT	Overlock 10
149	The Ln–Cu(II)–Hpic–H ₂ BDC system showing interesting production variety upon different reaction conditions: hydrothermal synthesis, structures, thermostability, and magnetism. Journal of Coordination Chemistry, 2010, 63, 1147-1156.	0.8	6
150	Water structure: A rare 3D water-chlorin architecture. Inorganic Chemistry Communication, 2011, 14, 1283-1285.	1.8	6

151	Thermodynamically stable MOF showing a highly rare four-connected hxg-d-4-Cccm net with self-penetration, polyrotaxane, and polycatenane multi-features. CrystEngComm, 2016, 18, 1693-1698.	1.3	6
152	Syntheses, Structures, and Magnetic Properties of a Series of Heterotri-, Tetra- and Pentanuclear LnIII–Coll Compounds. Polymers, 2019, 11, 196.	2.0	6
153	One metallic-organic framework with chain-like counterions and water molecules capsulated in the 1D chiral channels from the 2D 2-fold inclined interpenetrating (4,4) nets. Journal of Molecular Structure, 2007, 828, 162-165.	1.8	5
154	An unprecedented (3, 4)-connected self-penetrating metal–organic framework. Inorganic Chemistry Communication, 2014, 39, 90-93.	1.8	5
155	An unprecedented (4,8)-connected net featuring gsp2 topology and containing an exceptional coordination mode of acylamide ligand. CrystEngComm, 2014, 16, 5216.	1.3	5
156	A novel 4-connected binodal Moganite net with three-fold interpenetration. Inorganic Chemistry Communication, 2014, 39, 1-4.	1.8	5
157	A novel MOF showing a ring-like planar Zn ₆ cluster and the coexistence of a single, double, and triple wall. CrystEngComm, 2016, 18, 6336-6340.	1.3	5
158	Thhorium Metal–Organic Framework Showing Proton Transformation from [NH ₂ (CH ₃) ₂] ⁺ to the Carboxyl Group to Enhance Porosity for Selective Adsorption of D ₂ over H ₂ and Ammonia Capture. Crystal Growth and Design, 2020, 20, 3605-3610.	1.4	5
159	A highly rare 3D U-Cu metal-organic framework showing three-connected srs topology and nine-fold interpenetration. Inorganic Chemistry Communication, 2020, 119, 108041.	1.8	5
	2 (14 purezal 2 ul) purezing a politonia N dopor lizend used to construct (u. [2, 2] molecular gride		

160	2-(1H-pyrazol-3-yl)pyrazine: a polytopic N-donor ligand used to construct Cu-[2+2] molecular grid: synthesis, structure, and magnetic properties. Journal of Coordination Chemistry, 2012, 65, 104-111.	0.8	4
161	Two New One-Dimensional Homospin Dy(III) Compounds Showing Slow Magnetic Relaxation. Australian Journal of Chemistry, 2012, 65, 1436.	0.5	4

162An unprecedented T4(1)4(2)5(2) water topology. Inorganic Chemistry Communication, 2012, 15, 252-255.1.84

#	Article	IF	CITATIONS
163	In situ identification and absolute separation of small molecules by single crystal X-ray diffraction in metal–organic frameworks. CrystEngComm, 2016, 18, 5429-5433.	1.3	4
164	Luminescence modulation by twisting the branches of organic building blocks in uranyl-organic frameworks. Cell Reports Physical Science, 2022, , 100913.	2.8	4
165	A non-interpenetrating 3D porous metal-organic framework (MOF) holding rutile-type topology containing Cu4 secondary building units. Inorganic Chemistry Communication, 2012, 16, 43-46.	1.8	3
166	An unprecedented (3, 6)-connected net featuring tcj-3,6-P2 ₁ /c topology. RSC Advances, 2014, 4, 36282-36285.	1.7	3
167	A new acrylamide MOF with sra net showing an uncommon eight-fold interpenetration. Inorganic Chemistry Communication, 2014, 44, 29-31.	1.8	3
168	In-situ modification of trinuclear Mg 3 unit for modulating topology, porosity, and adsorption properties. Inorganic Chemistry Communication, 2016, 70, 181-184.	1.8	3
169	A 1D brick-like coordination polymer containing free-standing sulfonic units for luminescence sensing of uranium in aqueous solution. Journal of Solid State Chemistry, 2021, 299, 122153.	1.4	3
170	Highly stable Cd(II)-MOFs based on 2,6-naphthanlenedisulfonate and bisimidazole ligands: A new platform for selective detection of Cu2+ and efficient removal of iodine. Journal of Solid State Chemistry, 2021, 302, 122439.	1.4	3
171	A novel interdigitating metal-organic architecture showing the double edge-containing (4,4)topology based on the eight-connected Mn4 tetramer. Journal of Coordination Chemistry, 2007, 60, 1673-1680.	0.8	2
172	The synthesis, structure, and magnetic studies of one supramolecular <i>PtS</i> net. Journal of Coordination Chemistry, 2012, 65, 2705-2712.	0.8	2
173	A Complex Selfâ€Catenated Coordination Framework with a Rare (3,12)â€Connected Underlying Net Showing Selective Adsorption of CO ₂ . European Journal of Inorganic Chemistry, 2015, 2015, 4633-4637.	1.0	2
174	Innenrücktitelbild: Significant Enhancement of C ₂ H ₂ /C _{/C₂H₄ Separation by a Photochromic Diarylethene Unit: A Temperature―and Lightâ€Responsive Separation Switch (Angew. Chem. 27/2017). Angewandte Chemie, 2017, 129, 8127-8127.}	1.6	2
175	Unique magnetic behaviour of coexistence of single ion magnet and spin crossover. Inorganic Chemistry Communication, 2019, 102, 10-15.	1.8	2
176	Dual magnetic behavior of dysprosium(III) molecular magnet and Co(II) spin-crossover in an isolated [3d]-[4f] compound. Inorganic Chemistry Communication, 2019, 105, 93-96.	1.8	2
177	Multi-step Phase Transformation from Metal–Organic Frameworks to Inorganic Compounds for High-Purity Th(IV) Generation. Inorganic Chemistry, 2022, , .	1.9	1
178	One 2D Ni(II)-based compound showing diamagnetic-paramagnetic transition. Inorganic Chemistry Communication, 2012, 17, 68-70.	1.8	0
179	Synthesis, structure and luminescence properties of two new acylamide metal–organic frameworks showing 4-connected CdSO4and a threefold interpenetratingdianet. Acta Crystallographica Section C, Structural Chemistry, 2015, 71, 636-642.	0.2	0
180	Correction: Lanthanide separation using size-selective crystallization of Ln-MOFs. Chemical Communications, 2017, 53, 7100-7100.	2.2	0

#	Article	IF	CITATIONS
181	Rücktitelbild: The MOF ⁺ Technique: A Significant Synergic Effect Enables High Performance Chromate Removal (Angew. Chem. 51/2017). Angewandte Chemie, 2017, 129, 16636-16636.	1.6	0
182	Frontispiece: The MOF+ Technique: A Potential Multifunctional Platform. Chemistry - A European Journal, 2018, 24, .	1.7	0
183	U=O activation in uranyl-organic framework through solid-liquid reaction: A powerful tool to modulate electronic and magnetic structure. Journal of Solid State Chemistry, 2021, 298, 121948.	1.4	Ο
184	Applications of covalent organic framework–based nanomaterials as superior adsorbents in wastewater treatment. , 2022, , 127-159.		0
185	U–Co Bimetallic–Organic Framework Showing a Helical 1D Pore Decorated by Abundant â^'CH3 Groups: Robust Nature under Acid, Base, and Water for High-Performance SO2 Removal. Inorganic Chemistry, 2021, , .	1.9	0